J|A|C|S ARTICLES

Published on Web 08/10/2010

$Sc_2(\mu_2\text{-}O)$ Trapped in a Fullerene Cage: The Isolation and Structural Characterization of $Sc_2(\mu_2\text{-}O)@C_s(6)\text{-}C_{82}$ and the Relevance of the Thermal and Entropic Effects in Fullerene Isomer Selection

Brandon Q. Mercado,[†] Melissa A. Stuart,[‡] Mary A. Mackey,[‡] Jane E. Pickens,[‡] Bridget S. Confait,[‡] Steven Stevenson,*[,‡] Michael L. Easterling,[§] Ramón Valencia,[||] Antonio Rodríguez-Fortea,[||] Josep M. Poblet,*[,||] Marilyn M. Olmstead,*[,†] and Alan L. Balch*[,†]

Department of Chemistry, University of California, One Shields Avenue, Davis, California 95616, Department of Chemistry, University of Southern Mississippi, Hattiesburg, Mississippi 39406, Bruker Daltonics, Billerica, Massachusetts 01821, and Departament de Química Física i Inorgànica, Universitat Rovira i Virgili, c/Marcel·lí Domingo s/n, 43007 Tarragona, Spain

Received June 4, 2010; E-mail: albalch@ucdavis.edu; steven.stevenson@usm.edu; josepmaria.poblet@urv.cat

Abstract: The new endohedral fullerene, $Sc_2(\mu_2\text{-}O)@C_s(6)\text{-}C_{82}$, has been isolated from the carbon soot obtained by electric arc generation of fullerenes utilizing graphite rods doped with 90% Sc_2O_3 and 10% Cu (w/w). $Sc_2(\mu_2\text{-}O)@C_s(6)\text{-}C_{82}$ has been characterized by single crystal X-ray diffraction, mass spectrometry, and UV/vis spectroscopy. Computational studies have shown that, among the nine isomers that follow the isolated pentagon rule (IPR) for C_{82}, cage 6 with C_s symmetry is the most favorable to encapsulate the cluster at $T > 1200$ K. $Sc_2(\mu_2\text{-}O)@C_s(6)\text{-}C_{82}$ is the first example in which the relevance of the *thermal* and *entropic* contributions to the stability of the fullerene isomer has been clearly confirmed through the characterization of the X-ray crystal structure.

Introduction

Encapsulation of one guest molecule inside another host is a fascinating area of supramolecular chemistry that can lead to the stabilization of reactive guest molecules such as the elusive cyclobutadiene[1] and/or to alteration of their chemical reactivity as demonstrated recently for P_4.[2] Despite their relatively large size, the closed cages of carbon atoms known as fullerenes can act under suitable circumstances as either guests or hosts. As guests, fullerene cages may be found on the inside of carbon nanotubes where nanopeapods are formed.[3] In addition to the mechanical trapping of these cages within the nanotube walls, reactions between fullerenes, such as their fusion, have been observed.[4] Fullerenes can also act as hosts to form endohedral fullerenes, carbon cages with one or more atoms or molecules trapped on the inside. For example, when the prototypical fullerene, C_{60}, is prepared in an electrical arc utilizing a low-pressure helium atmosphere, one out every million C_{60} molecules formed traps a helium atom to produce the endohedral, $He@C_{60}$.[5]

Many other endohedral fullerenes that contain rare gas atoms, nitrogen or phosphorus atoms, or one, two, or even three electropositive metal atoms have been detected and in some cases isolated.[6] Additionally, endohedral fullerenes that trap one or two diatomic molecules (*e.g.*, $H_2@C_{60}$,[7] $N_2@C_{60}$,[8] $(H_2)_2@C_{70}$[9]) have been prepared. Another class of endohedral fullerenes contain clusters of metal atoms that surround one or more main group atoms. In this area, endohedral fullerenes containing the M_3N unit have attracted considerable attention,[10,11] in part because the prototypical $Sc_3N@I_h\text{-}C_{80}$ is the endohedral fullerene that is produced in highest quantity in the electric arc procedure for fullerene generation.[12] Extensive arrays of en-

[†] University of California.
[‡] University of Southern Mississippi.
[§] Bruker Daltonics.
[||] Universitat Rovira i Virgili.

(1) Cram, D. J.; Tanner, M. E.; Thomas, R. *Angew. Chem., Int. Ed.* **1991**, *30*, 1024–1027.
(2) Mal, P.; Breiner, B.; Rissanen, K.; Nitschke, J. R. *Science* **2009**, *324*, 1697–1699.
(3) Smith, B. W.; Monthioux, M.; Luzzi, D. E. *Nature* **1998**, *396*, 323–324.
(4) Chuvilin, A.; Khlobystov, A. N.; Obergfell, D.; Haluska, M.; Yang, S.; Roth, S.; Kaiser, U. *Angew. Chem., Int. Ed.* **2010**, *49*, 193–196.
(5) Saunders, M.; Jiménez-Vázquez, H. A.; Cross, R. J.; Poreda, R. J. *Science* **1993**, *259*, 1428–1430.
(6) Akasaka, T.; Nagase, S. *Endofullerenes: A New Family of Carbon Clusters*; Kluwer Academic Publishers: Dordrecht, The Netherlands, 2002.
(7) Komatsu, K.; Murata, M.; Murata, Y. *Science* **2005**, *307*, 238–240.
(8) Suetsuna, T.; Dragoe, N.; Harneit, W.; Weidinger, A.; Shimotani, H.; Ito, S.; Takagi, H.; Kitazawa, K. *Chem.—Eur. J.* **2002**, *8*, 5079–5083.
(9) Murata, M.; Maeda, S.; Morinaka, Y.; Murata, Y.; Komatsu, K. *J. Am. Chem. Soc.* **2008**, *130*, 15800–15801.
(10) Dunsch, L.; Yang, S. *Small* **2007**, *3*, 1298–1320.
(11) Chaur, M. N.; Melin, F.; Ortiz, A. L.; Echegoyen, L. *Angew. Chem., Int. Ed.* **2009**, *48*, 7514–7538.
(12) Stevenson, S.; Rice, G.; Glass, T.; Harich, K.; Cromer, F.; Jordan, M. R.; Craft, J.; Hadju, E.; Bible, R.; Olmstead, M. M.; Maitra, K.; Fisher, A. J.; Balch, A. L.; Dorn, H. C. *Nature* **1999**, *401*, 55–57.

 10.1021/ja104902e

dohedrals that contain various metal acetylide units (M_2C_2,[13−16] M_3C_2,[17] M_4C_2,[18]) have been characterized, and there is one report of the trapping of a hydrocarbon fragment within an endohedral ($Sc_3CH@C_{80}$).[19]

Recently, the isolation and crystallographic characterization of two endohedral fullerenes that contained metal oxide fragments trapped inside an I_h-C_{80} cage were reported.[20,21] In $Sc_4(\mu_3\text{-}O)_2@I_h\text{-}C_{80}$, the four scandium ions form an imperfect tetrahedron that is bridged on two faces by oxide ions, while, in $Sc_4(\mu_3\text{-}O)_3@I_h\text{-}C_{80}$, the nearly tetrahedral array of four scandium ions is bridged on three faces by oxide ions. Computational studies on these clusters have indicated that the electronic distributions for the two endohedrals are $(Sc^{3+})_2(Sc^{2+})_2(O^{2-})_2@(I_h\text{-}C_{80}{}^{6-})$ and $(Sc^{3+})_4(O^{2-})_3@(I_h\text{-}C_{80}{}^{6-})$ and that the HOMOs in each are markedly different. In the mixed oxidation state cluster in $Sc_4(\mu_3\text{-}O)_2@I_h\text{-}C_{80}$, the HOMO is largely confined to the $Sc_4(\mu_3\text{-}O)_2$ unit, while, in $Sc_4(\mu_3\text{-}O)_3@I_h\text{-}C_{80}$, the HOMO is largely delocalized over the fullerene carbon atoms.[22,23]

Recent work has shown that M_2S units can also be trapped within fullerene cages. Dunsch and co-workers have reported the preparation of a series of endohedrals, $M_2S@C_{3v}(8)\text{-}C_{82}$, with M = Sc, Y, Dy, and Lu.[24] The sulfur source in this work was guanidinium thiocyanate, which is incorporated along with a metal oxide into the graphite rods used for fullerene formation. In a related study, Echegoyen and co-workers reported the formation of a series of scandium-based endohedrals, $Sc_2S@C_{2n}$ where $2n$ ranged from 82 to 100.[25] In this case, the sulfur source was sulfur dioxide, which was added to the helium atmosphere used for fullerene generation. It is interesting to note that this process results in the incorporation of hard scandium and the soft sulfur, rather than the hard and more abundant oxygen, into the resulting endohedral fullerene. In contrast to the results of Dunsch and co-workers, two isomers of $Sc_2S@C_{82}$ were separated and identified as utilizing the $C_{3v}(8)\text{-}C_{82}$ (as reported by Dunsch and co-workers) and $C_s(6)\text{-}C_{82}$ cages. The authors concluded that the sulfur source influenced the choice of fullerene cage isomer found in these new endohedrals.

Here, we report the discovery of another scandium oxide containing endohedral: $Sc_2(\mu_2\text{-}O)@C_s(6)\text{-}C_{82}$ that is formed in the same process that makes $Sc_4(\mu_3\text{-}O)_2@I_h\text{-}C_{80}$ and $Sc_4(\mu_3\text{-}O)_3@I_h\text{-}C_{80}$. The $Sc_2(\mu_2\text{-}O)$ and $Sc_2(\mu_2\text{-}S)$ units are valence isoelectronic. Hence, endohedrals containing these fragments should be closely related. Computational studies have been performed to evaluate the stabilities of the $Sc_2(\mu_2\text{-}O)@C_s(6)\text{-}C_{82}$ and $Sc_2(\mu_2\text{-}O)@C_{3v}(8)\text{-}C_{82}$ isomers.

Results

Preparation and Purification of $Sc_2(\mu_2\text{-}O)@C_s(6)\text{-}C_{82}$. Carbon soot was prepared in an electric-arc reactor, with carbon rods that contained a core of 90% Sc_2O_3 and 10% Cu (w/w).[26] The soot was extracted with carbon disulfide, and the endohedral fullerenes were removed from solution in two successive stages by precipitation with aluminum(III) chloride. Figure 1 shows the progress of the separation process. Parts (a) and (e) show the HPLC chromatogram and the MALDI mass spectrum of the extract from the raw soot. $Sc_3N@C_{78}$ and $Sc_2(\mu_2\text{-}O)@C_s(6)\text{-}C_{82}$ have similar retention times, and a chromatographic separation was not feasible. Consequently, precipitation of the endohedral fullerenes by treatment with aluminum(III) chloride was employed as a separation technique.[27] Parts (b) and (f) show that the initial precipitation step removed $Sc_4O_2@C_{80}$, $Sc_3N@C_{78}$, and the two isomers of $Sc_3N@C_{80}$ from solution, while parts (c) and (g) indicate that the second treatment with aluminum(III) chloride resulted in the precipitation of the desired $Sc_2(\mu_2\text{-}O)@C_s(6)\text{-}C_{82}$. The sample was subsequently purified by HPLC that utilized a semipreparative PYE column with toluene as eluent. Parts (d) and (h) of Figure 1 show the HPLC chromatogram and the MALDI mass spectrum of the purified sample of $Sc_2(\mu_2\text{-}O)@C_s(6)\text{-}C_{82}$.

For the determination of the molecular formula, a sample of $Sc_2(\mu_2\text{-}O)@C_s(6)\text{-}C_{82}$ was analyzed by high-resolution mass spectrometry. This experimental MALDI data and corresponding theoretical values are compared and summarized in Table 1. These experimental m/z values are consistent with theoretical predictions for the M, M+1, M+2, and M+3 peaks.

The UV/vis absorption spectrum of $Sc_2(\mu_2\text{-}O)@C_s(6)\text{-}C_{82}$ is shown in Figure 2. The spectrum, which shows four bands in the visible range with a particularly strong absorption at 500 nm, is similar to that of the initially eluting isomer $(Y_2C_2)@C_{82}(I)$.[13] The spectrum of $Sc_2(\mu_2\text{-}O)@C_s(6)\text{-}C_{82}$ is clearly different from that of $(Y_2C_2)@C_{82}(III)$ which has been shown to involve the $C_{3v}(8)\text{-}C_{82}$ cage.[13] The spectrum is also different from that of $Sc_2S@C_{3v}(8)\text{-}C_{82}$ but is similar to that of $Sc_2S@C_s(6)\text{-}C_{82}$.[25]

Structure of $Sc_2(\mu_2\text{-}O)@C_s(6)\text{-}C_{82}$ as Determined by Single Crystal X-ray Diffraction. Crystals for X-ray diffraction were obtained by slow diffusion of a benzene solution of $Ni^{II}(OEP)$ into a benzene solution of the purified endohedral followed by gradual evaporation until the sample was nearly dry. Figure 3 shows the structure of the endohedral fullerene and its relationship to the nickel porphyrin. For a C_{82} cage there are 9 isomers (three different C_2 isomers, three C_s isomers, two C_{3v} isomers, and one C_{2v} isomer) that follow the isolated pentagon rule (IPR). The crystallographic data clearly indicate that the $C_s(6)\text{-}C_{82}$

(13) Inoue, T.; Tomiyama, T.; Sugai, T.; Okazaki, T.; Suematsu, T.; Fujii, N.; Utsumi, H.; Nojima, K.; Shinohara, H. *J. Phys. Chem. B* **2004**, *108*, 7573–7579.
(14) Wang, C. R.; Kai, T.; Tomiyama, T.; Yoshida, T.; Kobayashi, Y.; Nishibori, E.; Takata, M.; Sakata, M.; Shinohara, H. *Angew. Chem., Int. Ed.* **2001**, *40*, 397–399.
(15) Shi, Z. Q.; Wu, X.; Wang, C. R.; Lu, X.; Shinohara, H. *Angew. Chem., Int. Ed.* **2006**, *45*, 2107–2111.
(16) Yang, H.; Lu, C.; Liu, Z.; Jin, H.; Che, Y.; Olmstead, M. M.; Balch, A. L. *J. Am. Chem. Soc.* **2008**, *130*, 17296–17300.
(17) Iiduka, Y.; Wakahara, T.; Nakahodo, T.; Tsuchiya, T.; Sakuraba, A.; Maeda, Y.; Akasaka, T.; Yoza, K.; Horn, E.; Kato, T.; Liu, M. T. H.; Mizorogi, N.; Kobayashi, K.; Nagase, S. *J. Am. Chem. Soc.* **2005**, *127*, 12500–12501.
(18) Wang, S.-T.; Chen, N.; Xiang, J.-F.; Li, B.; Wu, J.-Y.; Xu, W.; Jiang, L.; Tan, K.; Shu, C.-Y.; Lu, X.; Wang, C.-R. *J. Am. Chem. Soc.* **2009**, *131*, 16646–16647.
(19) Krause, M.; Ziegs, F.; Popov, A. A.; Dunsch, L. *ChemPhysChem* **2007**, *8*, 537–540.
(20) Stevenson, S.; Mackey, M. A.; Stuart, M. A.; Philips, J. P.; Easterling, M. L.; Chancellor, C. J.; Olmstead, M. M.; Balch, A. L. *J. Am. Chem. Soc.* **2008**, *130*, 11844–11845.
(21) Mercado, B. Q.; Olmstead, M. M.; Beavers, C. M.; Easterling, M. L.; Stevenson, S.; Mackey, M. A.; Coumbe, C. E.; Phillips, J. D.; Phillips, J. P.; Poblet, J. M.; Balch, A. L. *Chem. Commun.* **2010**, *46*, 279–281.
(22) Valencia, R.; Rodriguez-Fortes, A.; Stevenson, S.; Balch, A. L.; Poblet, J. M. *Inorg. Chem.* **2009**, *48*, 5957.
(23) Popov, A. A.; Dunsch, L. *Chem.—Eur. J.* **2009**, *15*, 9707–9729.
(24) Dunsch, L.; Yang, S.; Zhang, L.; Svitova, A.; Oswald, S.; Popov, A. A. *J. Am. Chem. Soc.* **2010**, *132*, 5413–5421.
(25) Chen, N.; Chaur, M. N.; Moore, C.; Pinzon, J. R.; Valencia, R.; Rodríguez-Fontea, A.; Poblet, J. M.; Echegoyen, L. *Chem. Commun.* **2010**, *46*, 4818–4820.
(26) Stevenson, S.; Mackey, M. A.; Thompson, M. C.; Coumbe, H. L.; Madasu, P. K.; Coumbe, C. E.; Phillips, J. P. *Chem. Commun.* **2007**, 4263–4265.
(27) Stevenson, S.; Mackey, M. A.; Pickens, J. E.; Stuart, M. A.; Confait, B. S.; Phillips, J. P. *Inorg. Chem.* **2009**, *48*, 11685–11690.

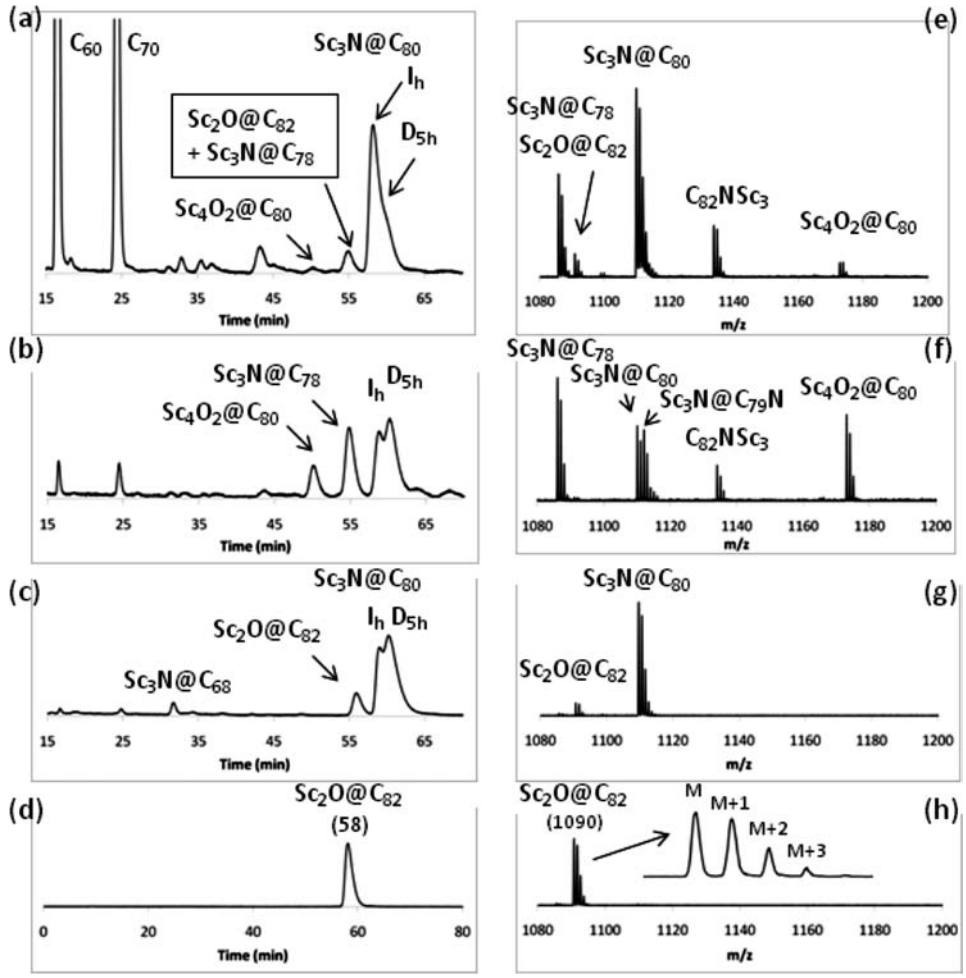

Figure 1. HPLC chromatograms of (a) fullerene extract, (b,c) metallofullerenes selectively precipitated with $AlCl_3$, (b) stage 1 and (c) stage 2, and (d) HPLC purified $Sc_2(\mu_2\text{-}O)@C_s(6)\text{-}C_{82}$. Chromatographic conditions for (a−c) include a 4.6 mm × 250 mm PYE column, 0.3 mL/min toluene mobile phase, 360 nm UV detection, and 50 μL injection, and those for (d) include a 10 mm × 250 mm PYE column and 1.5 mL/min toluene. (e−h) MALDI spectra corresponding to (a−d), respectively.

Table 1. Experimental and Computed Mass for $Sc_2(\mu_2\text{-}O)@C_s(6)\text{-}C_{82}$ from High-Resolution Mass Spectrometry

Peak	Theoretical	Experimental
$Sc_2O@C_{82}$ (M)	1089.90619	1089.90786
$Sc_2O@C_{82}$ (M+1)	1090.90954	1090.91134
$Sc_2O@C_{82}$ (M+2)	1090.91289	1091.91539
$Sc_2O@C_{82}$ (M+3)	1092.91625	1092.91918

isomer is present in this endohedral despite the fact that the fullerene cage is disordered. As is common in fullerene structures, the mirror plane of the carbon cage is not congruent with a crystallographic mirror plane. Additionally, there are two orientations of the cage with fractional occupancies of 0.824 and 0.176. Figure 3 was drawn so that the noncrystallographic mirror plane of the C_{82} cage lies perpendicular to the picture plane.

The Sc_2O unit inside the fullerene cage is also disordered. The major site shown in Figure 3 involves the set {Sc1, Sc2, O1} with 0.38 fractional occupancy. Within that unit, the Sc−O distances are 1.934(5) Å for Sc1 and 1.867(4) Å for Sc2, and the Sc1−O1−Sc2 angle is 156.6(3)°. However, in the asymmetric unit there are two sites for the oxide ion and eight fractionally occupied sites for the scandium ions. Figure 4 shows two orthogonal views that demonstrate how these sites are arranged inside the major orientation of the $C_s(6)\text{-}C_{82}$ cage. As

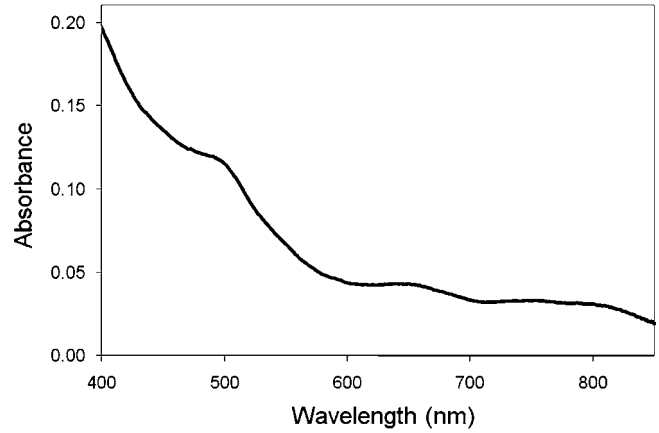

Figure 2. UV−vis spectrum of $Sc_2(\mu_2\text{-}O)@C_s(6)\text{-}C_{82}$ in CS_2 solution.

a result of this disorder, a precise description of the geometry of the Sc_2O unit is not forthcoming. It is well-known that $M_2(\mu\text{-}O)$ units in coordination complexes are flexible and can display significant variation in the M−O−M angle.[28] While the oxide ion sites are clustered near the center of the carbon cage, the

(28) Lee, H. M.; Olmstead, M. M.; Gross, G. G.; Balch, A. L. *Cryst. Growth Des.* **2003**, *3*, 691–697.

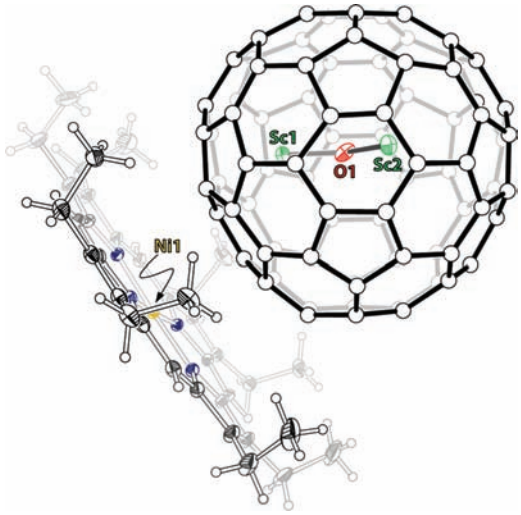

Figure 3. A view of the asymmetric unit in crystalline $Sc_2(\mu_2\text{-}O)@C_s(6)\text{-}C_{82}\cdot Ni^{II}(OEP)\cdot 1.4CH_3C_6H_5\cdot 0.6C_6H_6$ that shows the inter-relationship of the endohedral fullerene and the nickel porphyrin. Only the major sites for the cage $C_s(6)\text{-}C_{82}$ (fractional occupancy of 0.824) and the Sc_2O unit are shown.

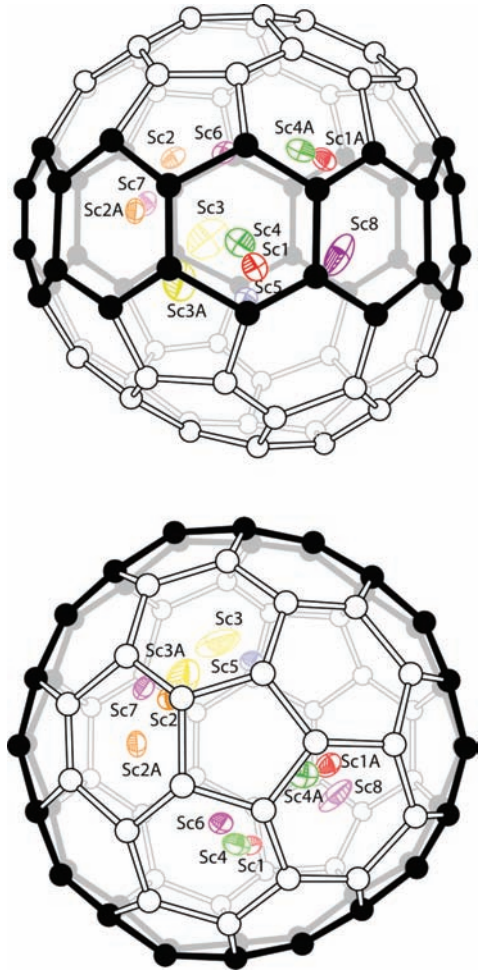

Figure 4. Two orthogonal views of $Sc_2(\mu_2\text{-}O)@C_s(6)\text{-}C_{82}$ that show the locations of the scandium ions along the set of 10 contiguous hexagons of the fullerene. The fractional site occupancies are as follows: Sc1, 0.54; Sc2, 0.38; Sc3, 0.30; Sc4, 0.28; Sc5, 0.24; Sc6, 0.16; Sc7, 0.06; Sc8, 0.04. Sites labeled A are generated by the crystallographic mirror plane.

scandium ion positions are arranged along the walls of the fullerene. The $C_s(6)\text{-}C_{82}$ cage possesses a unique band of 10 contiguous hexagons that is highlighted in Figure 4. As the figure shows, the scandium ions are located along that set of 10 contiguous hexagons. The arrangement of scandium ions along a band of hexagons is similar to the situation found in $Er_2@C_s(6)\text{-}C_{82}\cdot\{Co^{II}(OEP)\}\cdot 1.4(C_6H_6)\cdot 0.3(CHCl_3)$, where the two erbium ions are distributed between 23 different sites along the band of 10 contiguous hexagons on the fullerene inner surface.[29]

Table 2. Relative Stabilities for C_{82}, C_{82}^{4-}, and $Sc_2(\mu_2\text{-}O)@C_s(6)\text{-}C_{82}$[a]

	Isomer $C_s(6)$	Isomer $C_{3v}(8)$	Isomer $C_{2v}(9)$
ΔE (C_{82})[b]	0.0	15.0	3.1
ΔE (C_{82}^{4-})[b]	8.0	0.0	2.4
ΔE ($Sc_2O@C_{82}$)	3.8	0.0	7.9
ΔH ($Sc_2O@C_{82}$, 0 K)	3.1	0.0	7.3
ΔG ($Sc_2O@C_{82}$, 1000 K)	0.0	2.7	3.1

[a] Energies are in kcal·mol^{-1}. [b] Values taken from ref 30.

Computational Studies of the Electronic Structure of $Sc_2(\mu_2\text{-}O)@C_s(6)\text{-}C_{82}$ and Related Molecules. DFT calculations have been carried out on $Sc_2(\mu_2\text{-}O)@C_{82}$ for cages $C_s(6)$, $C_{3v}(8)$, and $C_{2v}(9)$. For each one of these endohedral fullerenes, we have analyzed a minimum of 10 orientations of the $Sc_2(\mu_2\text{-}O)$ moiety inside the carbon cage. The internal cluster may adopt several orientations within a small range of energy. Hence, for example, for isomer $C_{3v}(8)$, 13 orientational isomers have been analyzed, four of them appearing in a range lower than 1.5 kcal mol^{-1} (see Figure S2 in the Supporting Information). The rotation seems more hindered for isomers $C_s(6)$ and $C_{2v}(9)$, but in general we can assert that $Sc_2(\mu_2\text{-}O)$ can rotate quite freely inside the fullerene. DFT calculations predict isomer $C_{3v}(8)$ as the lowest-energy tetra-anion for an IPR fullerene with 82 carbon atoms (Table 2); isomers $C_{2v}(9)$ and $C_s(6)$ are the second and third most stable C_{82}^{4-} species. When neutral, isomer $C_s(6)$ is the lowest-energy isomer among these three cages. After encapsulation of $Sc_2(\mu_2\text{-}O)$, isomer $C_{3v}(8)$ becomes the lowest-energy species as expected from a formal charge transfer of four electrons. This finding, however, seems to be in contradiction with the characterization of isomer $C_s(6)$ for $Sc_2(\mu_2\text{-}O)@C_{82}$. We have checked that this result does not depend on the density functional; B3LYP predicts almost the same energy difference between cages 6 and 8 (4.1 kcal·mol^{-1}).

In order to evaluate the relevance of thermal and entropic contributions to the stability of these three isomers, we have also computed the free energies in the rigid rotor + harmonic oscillator approximation (RRHO) at different temperatures as well as their molar fractions derived from the free-energy calculations as done by Slanina and co-workers for many empty fullerenes[31] and some endohedral metallofullerenes.[32] The incorporation of the zero-point-energy correction to the electronic energy only reduces ΔE, the energy difference between isomers $C_s(6)$ and $C_{3v}(8)$, from 3.8 to 3.1 kcal·mol^{-1}. However, when the entropic and thermal effects are taken into account,

(29) Olmstead, M. M.; de Bettencourt-Dias, A.; Stevenson, S.; Dorn, H. C.; Balch, A. L. *J. Am. Chem. Soc.* **2002**, *124*, 4172–1473.
(30) Valencia, R.; Rodriguez-Fortea, A.; Poblet, J. M. *J. Phys. Chem. A* **2008**, *112*, 4550–4555.
(31) (a) Slanina, Z. *Int. Rev. Phys. Chem.* **1987**, *6*, 251–267. (b) Zhao, X.; Slanina, Z.; Goto, H.; Osawa, E. *J. Chem. Phys.* **2003**, *118*, 10534–10540. (c) Zhao, X.; Slanina, Z.; Goto, H. *J. Phys. Chem. A* **2004**, *108*, 4479–4484, and references therein.
(32) (a) Slanina, Z.; Nagase, S. *ChemPhysChem* **2005**, *6*, 2060–2063. (b) Slanina, Z.; Lee, S.-L.; Uhlík, F.; Adamowicz, L.; Nagase, S. *J. Comput. Methods. Sci. Eng.* **2006**, *6*, 243–250.

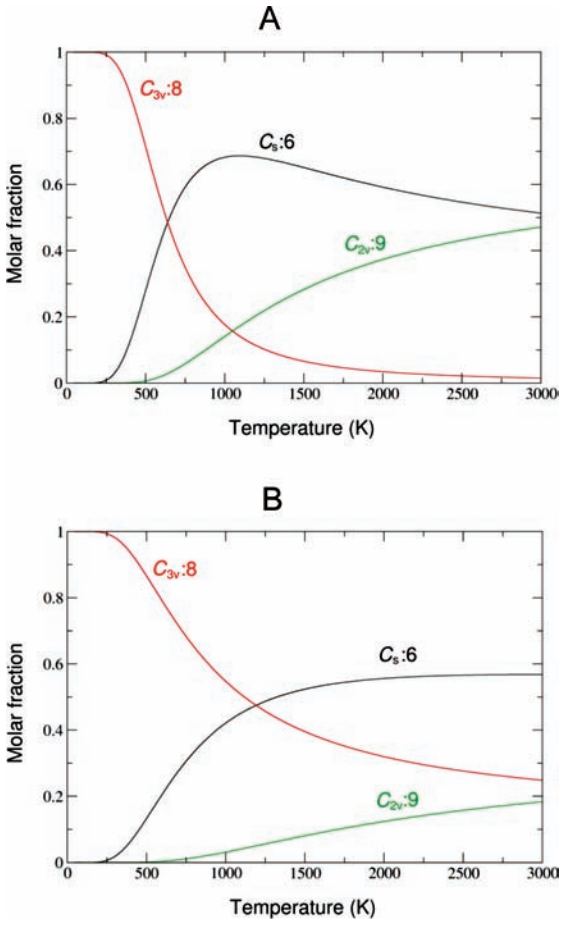

Figure 5. A plot of the computed molar fractions at (A) RRHO and (B) FEM approximations of the $Sc_2(\mu_2\text{-O})@C_{3v}(8)\text{-}C_{82}$, $Sc_2(\mu_2\text{-O})@C_s(6)\text{-}C_{82}$, and $Sc_2(\mu_2\text{-O})@C_{2v}(9)\text{-}C_{82}$ isomers as a function of the temperature of formation.

there is an inversion in their relative stabilities. For example, at 1000 K isomer $C_s(6)$ exhibits the smallest free energy. Consequently, $Sc_2(\mu_2\text{-O})@C_{3v}(8)\text{-}C_{82}$ is predicted to be the most abundant product at low temperatures, but $Sc_2(\mu_2\text{-O})@C_s(6)\text{-}C_{82}$ is more favored from an entropic point of view and becomes the most abundant species at higher temperatures as the molar fractions represented in Figure 5 show. The crossing temperature is computed to be ~640 K. A modified treatment based on the idea that the encapsulated atoms can exercise large amplitude motions, especially at high temperatures, was also used. In this approximation, which is called the free, fluctuating (or floating) encapsulate model (FEM),[33] the crossing of the molar fractions appears at higher temperature (~1200 K). The molar fraction of $Sc_2(\mu_2\text{-O})@C_{3v}(9)\text{-}C_{82}$ also increases at higher temperatures: the RRHO model predicts it to be the second most abundant isomer at $T > 1000$ K; however, within the FEM model, up to 3000 K, it is the less abundant isomer (Figure 5).

$Sc_2(\mu_2\text{-O})@C_s(6)\text{-}C_{82}$ is stabilized by the transfer of four electrons from the internal cluster to the carbon cage as shown clearly in the molecular diagram in Figure 6. The four electrons that reside in the two highest-occupied orbitals of Sc_2O, which have a Sc nature, are transferred to carbon cage orbitals. After the encapsulation of the $Sc_2(\mu_2\text{-O})$ cluster, the HOMO and LUMO orbitals are mainly delocalized over the carbon cages and the orbital gap is only 0.915 eV, somewhat smaller than the analogous gap found for the $C_{3v}(8)$ isomer, 1.214 eV (Table 3). It is well-known that the atomic charges provided by the Atoms in Molecules (AIM) Theory[34] are, in general, more ionic than the atomic charges provided by other methods. Popov et al. have analyzed many endohedral metallofullerenes in terms of the AIM theory.[35] The atomic charges computed for Sc_2O inside C_{82} cages are approximately +2.40 e, which is significantly smaller than the value of *ca.* +3.60 e computed for $Sc_3N@I_h(7)\text{-}C_{80}$ or $Sc_4O_3@I_h(7)\text{-}C_{80}$, where the formal electron transfer is 6. In all of these compounds, the positive charge supported by each metal is very similar (between 1.76 and 1.80 e). In $Sc_4(\mu_3\text{-O})_3@I_h(7)\text{-}C_{80}$ two of the Sc atoms are not fully oxidized, and therefore the computed atomic charges for these two atoms are smaller (~1.44 e).

Discussion

There are nine isomers (three C_2 isomers, three C_s isomers, two C_{3v} isomers, and one C_{2v} isomer) of the C_{82} cage that obey the isolated pentagon rule (IPR), which requires that each of the 12 pentagons in a fullerene be surrounded by hexagons.[36] If the IPR is violated, as can occur for endohedral fullerenes,[37,38] then there are 39 710 possible isomers for C_{82} with surfaces comprised of only pentagons and hexagons. Empty cage C_{82} is formed in much lower abundance than C_{84}, C_{78}, and C_{76}, which are the most abundant of the simple fullerenes larger than C_{70}. ^{13}C NMR studies of samples of C_{82} have shown that three isomers with C_2, C_{2v}, and C_s symmetry are present in an 8:1:1 ratio.[39] The most abundant of these isomers, $C_2(3)\text{-}C_{82}$, has only recently been obtained in pure form.[40] Numerous endohedral fullerenes with C_{82} cages have been prepared, and a number of these have been structurally characterized. The major and minor isomers of $La@C_{82}$, which was the first endohedral to be isolated, have IPR-obeying cage structures with C_{2v}[41] and C_s[42] symmetry, respectively. The C_{2v} structure appears to be established for a number of other endohedrals of the $M@C_{82}$ type (M = Y, Ca, etc.),[43] but for $Ca@C_{82}$ three other isomers with C_s, C_{3v}, and C_2 symmetry have also been separated and characterized by ^{13}C NMR spectroscopy.[44] The structures of two of the three known isomers of $Er_2@C_{82}$ have been crystallographically characterized and shown to have the IPR-

(33) Slanina, Z.; Lee, S.-L.; Uhlík, F.; Nagase, S. *Theor. Chem. Acc.* **2007**, *117*, 315–322.
(34) Bader, R. F. W. *Atoms in Molecules. A Quantum Theory*; Clarendon Press: Oxford, 1990.
(35) Popov, A. A.; Dunsch, L. *Chem.—Eur. J.* **2009**, *15*, 9707–9729.
(36) Fowler, P. W.; Manolopoulos, D. E. *An Atlas of Fullerenes*; Clarendon Press: Oxford, 1995.
(37) Olmstead, M. M.; Lee, H. M.; Duchamp, J. C.; Stevenson, S.; Marciu, D.; Dorn, H. C.; Balch, A. L. *Angew. Chem., Int. Ed.* **2003**, *42*, 900–903.
(38) Beavers, C. M.; Zuo, T.; Duchamp, J. C.; Harich, K.; Dorn, H. C.; Olmstead, M. M.; Balch, A. L. *J. Am. Chem. Soc.* **2006**, *128*, 11352–11353.
(39) Kikuchi, K.; Nakahara, N.; Wakabayashi, T.; Suzuki, S.; Shiromaru, H.; Miyake, Y.; Saito, K.; Ikemoto, I.; Kainosho, M.; Achiba, Y. *Nature* **1992**, *357*, 142–145.
(40) Zalibera, M.; Popov, A. A.; Kalbac, M.; Rapta, P.; Dunsch, L. *Chem.—Eur. J.* **2008**, *14*, 9960–9967.
(41) (a) Akasaka, T.; et al. *J. Am. Chem. Soc.* **2000**, *122*, 9316–9317. (b) Feng, L.; Tsuchiya, T.; Wakahara, T.; Nakahodo, T.; Piao, Q.; Maeda, Y.; Akasaka, T.; Kato, T.; Yoza, K.; Horn, E.; Mizorogi, N.; Nagase, S. *J. Am. Chem. Soc.* **2006**, *128*, 5990–5991.
(42) Akasaka, T.; Wakahara, T.; Nagase, S.; Kobayashi, K.; Waelchli, M.; Yamamoto, K.; Kondo, M.; Shirakura, S.; Maeda, Y.; Kato, T.; Kako, M.; Nakadaira, Y.; Gao, X.; Van Caemelbecke, E.; Kadish, K. M. *J. Phys. Chem. B* **2001**, *105*, 2971–2974.
(43) Feng, L.; Wakahara, T.; Tsuchiya, T.; Maeda, Y.; Lian, Y.; Akasaka, T.; Mizorogi, N.; Kobayashi, K.; Nagase, S.; Kadish, K. M. *Chem. Phys. Lett.* **2005**, *405*, 274–277.

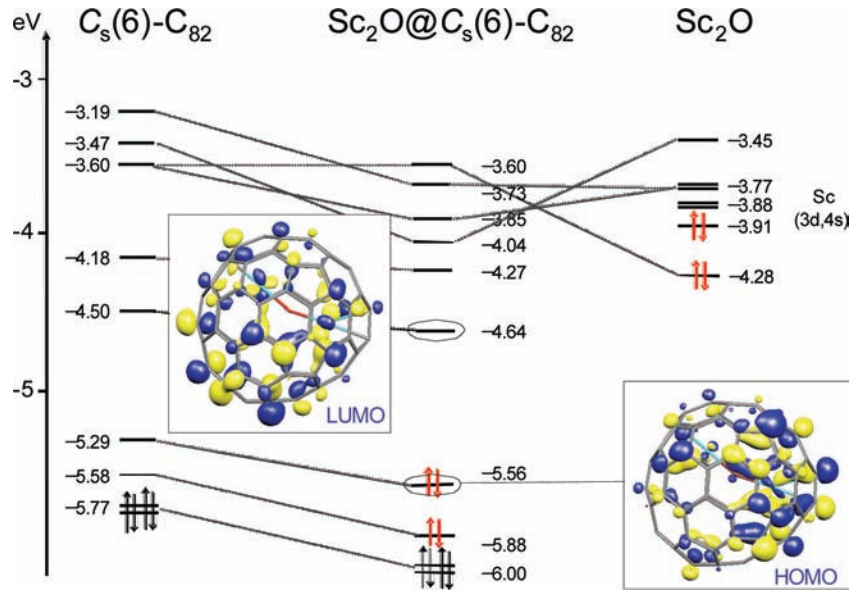

Figure 6. Molecular orbital diagram for $Sc_2(\mu_2\text{-}O)@C_s(6)\text{-}C_{82}$. The fragments, $Sc_2(\mu_2\text{-}O)$ and $C_s(6)\text{-}C_{82}$, were calculated with the geometry that they have in the endohedral fullerene.

Table 3. Orbital Energies and Bader (AIM) Charges for Several Endohedral Metallofullerenes[a]

	q(Sc)	q(O/N)	$q(C_{80}/C_{82})$	HOMO	LUMO	H−L gap
$Sc_2(\mu_2\text{-}O)@C_s(6)\text{-}C_{82}$	+1.785	−1.178	−2.392	−5.558	−4.643	0.915
$Sc_2(\mu_2\text{-}O)@C_{3v}(8)\text{-}C_{82}$	+1.795	−1.172	−2.417	−5.708	−4.494	1.214
$Sc_4(\mu_3\text{-}O)_2@I_h(7)\text{-}C_{80}$	+1.441 +1.752	−1.250	−3.886	−5.192	−4.593	0.599
$Sc_4(\mu_3\text{-}O)_3@I_h(7)\text{-}C_{80}$	+1.800	−1.205	−3.583	−5.886	−4.403	1.483
$Sc_3N@I_h(7)\text{-}C_{80}$	+1.765	−1.654	−3.642	−5.808	−4.463	1.345

[a] Energies in eV and charges in e.

obeying structures: $Er_2@C_s(6)\text{-}C_{82}$[45] and $Er_2@C_{3v}(8)\text{-}C_{82}$.[46] The carbide-containing endohedral, $Sc_2C_2@C_{82}$, utilizes the IPR-obeying cage with $C_{3v}(8)$ symmetry,[47] and the three isomers of $Y_2C_2@C_{82}$ have been shown by ^{13}C NMR spectra to have cages that follow the IPR with C_s, $C_{2v}(9)$, and $C_{3v}(8)$ symmetries.[13] In contrast, $Gd_3N@C_s(39663)\text{-}C_{82}$ does not follow the IPR but has a cage structure that has one site where two pentagons abut.[48]

The gaseous suboxide, Sc_2O, has been previously identified in mass spectrometric studies of the reaction between scandium metal and scandium oxide, and the Sc−O distance was estimated as 1.72 Å.[49] In contrast, the $(Sc_4(\mu_3\text{-}O)_2)^{6+}$ and $(Sc_4(\mu_3\text{-}O)_3)^{6+}$ clusters found in $Sc_4(\mu_3\text{-}O)_2@I_h\text{-}C_{80}$ and $Sc_4(\mu_3\text{-}O)_3@I_h\text{-}C_{80}$ have no precedent in the known chemical behavior of scandium. The stable oxide of scandium is the ionic solid Sc_2O_3, which was the starting material employed in the present study. The other known oxides of scandium, Sc_2O, ScO, and ScO_2, have only been detected in the gas phase.[50]

The prediction of the relative stability of cage isomers of endohedral metallofullerenes has been mainly based on the electronic properties of the host cage[51,52] with the assumption of an ionic model for these compounds.[53] In general, entropic and thermal contributions have not been considered, albeit Slanina and co-workers have already alleged their relevance.[31−33] From an electronic point of view, isomer $C_{3v}(8)$ is the most favorable IPR cage for the tetra-anions C_{82}^{4-}, but the difference of stability for endohedral metallofullerenes can be significantly altered after the encapsulation of a metal cluster. To the best of our knowledge $Sc_2O@C_s(6)\text{-}C_{82}$ is the first case where the crystallographically characterized structure of the major isomer (in this case the sole isomer) of a endohedral fullerene does not correspond to the most stable endohedral fullerene at 0 K. However, the two models proposed previously by Slanina predict isomer $C_s(6)$ as the most abundant product in the range of temperatures in which the endohedral metallofullerenes are formed.

It is informative to consider the related situation involving the two isomers of $La@C_{82}$. Computational studies show that the $C_{2v}(9)$ isomer is favored at 0 K[54] but that $C_s(6)$ and $C_{3v}(8)$ isomers become increasingly stable as the temperature of formation is increased.[33] Computations using the RRHO treatment predict that the $C_{3v}(8)$ isomer becomes increasingly prominent as the temperature increases, while calculations using the FEM treatment suggest that the $C_s(6)$ isomer is favored at high temperature. The major isomer of $La@C_{82}$ is $La@C_{2v}(9)\text{-}C_{82}$,[41] the isomer that is favored at 0 K, but there is a significant

(44) Kadama, T.; Fujii, R.; Miyake, Y.; Sakaguchi, K.; Nishikawa, H.; Ikemoto, I.; kikuchi, K.; Achiba, Y. *Chem. Phys. Lett.* **2003**, *377*, 197–200.
(45) Olmstead, M. M.; de Bettencourt-Dias, A.; Stevenson, S.; Dorn, H. C.; Balch, A. L. *J. Am. Chem. Soc.* **2002**, *124*, 4172–4173.
(46) Olmstead, M. M.; Lee, H. M.; Stevenson, S.; Dorn, H. C.; Balch, A. L. *Chem. Commun.* **2002**, 2688–2689.
(47) (a) Iiduka, Y.; Wakahara, T.; Nakajima, K.; Nakahodo, T.; Tsuchiya, T.; Maeda, Y.; Akasaka, T.; Yoza, K.; Liu, M. T. H.; Mizorogi, N.; Nagase, S. *Angew. Chem., Int. Ed.* **2007**, *46*, 5562–5564. (b) Iiduka, Y.; Wakahara, T.; Nakajima, K.; Tsuchiya, T.; Nakahodo, T.; Maeda, Y.; Akasaka, T.; Mizorogi, N.; Nagase, S. *Chem. Commun.* **2006**, 2057–2059.
(48) Mercado, B. Q.; Beavers, C. M.; Olmstead, M. M.; Chaur, M. N.; Walker, K.; Holloway, B. C.; Echegoyen, L.; Balch, A. L. *J. Am. Chem. Soc.* **2008**, *130*, 7854–7855.
(49) Smoes, S.; Drowart, J.; Verhaegen, G. *J. Chem. Phys.* **1965**, *43*, 732–736.
(50) Clemmer, D. E.; Dalleska, N. F.; Armentrout, P. B. *Chem. Phys. Lett.* **1992**, *190*, 259–265.
(51) Campanera, J. M.; Bo, C.; Poblet, J. M. *Angew. Chem., Int. Ed.* **2005**, *44*, 7230–7233.
(52) Popov, A. A.; Dunsch, L. *J. Am. Chem. Soc.* **2007**, *129*, 11835–11849.
(53) Chaur, M. N.; Valencia, R.; Rodriguez-Fortea, A.; Poblet, J. M.; Echegoyen, L. *Angew. Chem., Int. Ed.* **2009**, *48*, 1425–1429.
(54) Kobayashi, K.; Nagase, S. *Chem. Phys. Lett.* **1998**, *282*, 325–329.

amount of a minor isomer, which has been identified as La@C_s(6)-C_{82}.[42]

In the C_{80} family of endohedral fullerenes, computations have been performed to examine the relative stability of isomers for La@C_{80}. With the transfer of three electrons to the C_{80} cage, the C_{2v}(5), D_{5h}(6), and I_h(7) cage isomers are highly stabilized.[55] However, crystallographic studies on a *functionalized* adduct of La@C_{80} show that its cage structure is based upon the C_{2v}(3) isomer. Unfortunately, there are no computational studies that examine the effect of temperature on the stability of this unexpected isomer, and the contribution of the functionalization to the stability of this particular isomer is also unknown. Additional uncertainty surrounds the question of how functionalization might determine the fullerene that is extracted from the otherwise insoluble material from which the La@C_{80} adduct was obtained.

Our computational results are also relevant to providing an explanation for the fact that Dunsch and co-workers observed the exclusive formation of $Sc_2S@C_{3v}$(8)-C_{82},[24] whereas Echegoyen and co-workers reported the formation of both $Sc_2S@C_s$(6)-C_{82} and $Sc_2S@C_{3v}$(8)-C_{82}.[25] While the chemical source of the sulfur, which differed in the two arcing processes, may have influenced the course of fullerene formation, it may also have altered the temperature at which crucial aspects of fullerene synthesis occurred. Additionally, it should be realized that comparisons of fullerene isomer formation from different reactors operating under different conditions may overlook important variations in arc temperature. Likewise, the arc temperature and temperature gradient in our synthesis may contribute to the formation of only a single isomer rather than the two related isomers seen in the work of Echegoyen and co-workers.

In summary, a new endohedral fullerene, $Sc_2(\mu_2\text{-O})@C_s$(6)-C_{82}, has been isolated and characterized by mass spectrometry and UV/vis spectroscopy. The single crystal X-ray diffraction study clearly identifies the presence of the C_s(6)-C_{82} cage isomer and shows that a bent $Sc_2(\mu_2\text{-O})$ unit is disordered within this fullerene cage. Computational studies have shown that among the nine isomers of C_{82} that follow the isolated pentagon rule (IPR), cage 6 with C_s symmetry is the most favorable to encapsulate the cluster at $T > 1200$ K. $Sc_2(\mu_2\text{-O})@C_s$(6)-C_{82} is a particularly clear case where the relevance of the *thermal* and *entropic* contributions to the stability of the fullerene isomer has been confirmed through the characterization of the endohedral by X-ray diffraction.

Experimental Section

Preparation and Isolation of $Sc_2(\mu_2\text{-O})@C_s$(6)-C_{82}. Carbon soot containing fullerenes and endohedral fullerenes was prepared in an electric-arc reactor, in which a core-drilled, graphite rod containing a mixture of 90% Sc_2O_3 and 10% Cu (w/w) was vaporized.[26] The soot was collected, extracted with carbon disulfide, and filtered through a PTFE membrane. Upon solvent removal, the resulting dry fullerene extract was washed with diethyl ether and acetone to remove nonfullerene hydrocarbon-containing material. A 1.3 g portion of the extract was dissolved in 1.0 L of carbon disulfide. While the solution was stirring, 250 mg of $AlCl_3$ were added. During the 16.5 h of reaction time, the most reactive metallofullerenes precipitated from solution. The solution was filtered, the precipitate (stage 1 precipitate) was removed from solution by filtration, and the filtrate, which contained the desired $Sc_2(\mu_2\text{-O})@C_s$(6)-C_{82}, was treated with an additional 250 mg of $AlCl_3$. The reaction progress was monitored by injecting aliquots collected at arbitrary times to monitor the loss of the HPLC peak due to $Sc_2O@C_{82}$ (retention time, 55 min). After 6.5 h of reaction time, the desired $Sc_2(\mu_2\text{-O})@C_s$(6)-C_{82} along with $Sc_3N@D_{5h}$-C_{80} had precipitated. The reaction mixture was filtered to yield a black solid (stage 2 precipitate).

After filtration, the stage 1 and stage 2 precipitates were placed in separate separatory funnels that contained 20 mL of a saturated $NaHCO_3$ solution, ice chips, and ice water (10% vol) and CS_2 (90% vol) for decomplexation of the metallofullerenes and subsequent release of unfunctionalized metallofullerenes to the CS_2 layer. After two further washes with distilled water, the CS_2 layers were filtered though a membrane. Upon solvent removal and washing with diethyl ether, 75 mg of a black solid were obtained from the stage 1 precipitate, and 40 mg of another black solid were obtained from the stage 2 precipitate. Each of these two samples was dissolved in toluene. The corresponding HPLC and MALDI data for the solution obtained from the stage 1 precipitate are shown in parts b and f of Figure 1 and demonstrate the removal of significant amounts of $Sc_4O_2@C_{80}$, $Sc_3N@C_{78}$, and both isomers of $Sc_3N@C_{80}$. The corresponding HPLC and MALDI data for the solution obtained from the stage 2 precipitate are shown in parts c and g of Figure 1. At this point, the sample contains the desired $Sc_2O@C_{82}$ along with $Sc_3N@C_{68}$ and two isomers of $Sc_3N@C_{80}$. Since the MALDI data indicate the successful removal of the coeluting $Sc_3N@C_{78}$, this sample was amenable for HPLC separation. Repeated injections of a toluene solution of the stage 2 precipitate onto a semi-preparative PYE column permitted the collection of a purified sample of $Sc_2(\mu_2\text{-O})@C_s$(6)-C_{82}. The corresponding HPLC and MALDI data for the purified $Sc_2(\mu_2\text{-O})@C_s$(6)-C_{82} are shown in parts d and h of Figure 1.

Crystallographic Data Collection and Refinement for $Sc_2(\mu_2\text{-O})@C_s$(6)-$C_{82}\cdot$Ni(OEP)$\cdot 1.4CH_3C_6H_5\cdot 0.6C_6H_6$. Crystals were obtained by layering a solution of Ni(OEP) in benzene over a benzene solution of $Sc_2(\mu_2\text{-O})@C_s$(6)-C_{82} and allowing the sample to slowly mix and evaporate. Crystals formed only after nearly all the solvent had evaporated. Although benzene was used as the solvent for crystal growth, toluene, which was utilized in the sample purification, must have been entrained in the sample of the endohedral, since it was found as a component in the crystalline solid. A black block of dimensions 0.14 mm × 0.015 mm × 0.029 mm was mounted in the 90(2) K nitrogen cold stream provided by an Oxford Cryostream low temperature apparatus on the goniometer head of a Bruker D8 diffractometer equipped with an ApexII CCD detector, on beamline 11.3.1 at the Advanced Light Source in Berkeley, CA. Diffraction data were collected using synchrotron radiation monochromated with silicon(111) to a wavelength of 0.77490 Å. An approximate full sphere of data to $2\theta = 83.6°$ was collected using 0.3° ω scans. A multiscan absorption correction was applied using the program SADABS-2008/1.[56] A total of 144 527 reflections were collected, of which 20 400 were unique [R(int) = 0.055] and 17 273 were observed [$I > 2\sigma(I)$]. The structure was solved by direct methods (SHELXS97) and refined by full-matrix least-squares on F^2 (SHELXL97)[56] using 1202 parameters and 2807 restraints.

The C_{82} cage has two orientations: both are disordered with respect to the crystallographic mirror plane. The occupancies of these two orientations refined to 0.412(2) and 0.088(2). These occupancies sum to 0.5, where the remaining electron density is generated by the crystallographic mirror plane, and were subsequently fixed at these values.

Same distance restraints (SADI 0.01) were applied to all of the C−C bonds of the C_{82} molecule that are equivalent by the C_s point group. This creates 68 restraints. In addition, similarity restraints (SIMU) were applied to the anisotropic thermal parameters of the C_{82} cage, and these provided another 2739 restraints.

(55) Nikawa, H.; Yamada, T.; Cao, B.; Mizorogi, N.; Slanina, Z.; Tsuchiya, T.; Akasaka, T.; Yoza, K.; Nagase, S. *J. Am. Chem. Soc.* **2009**, *131*, 10950–190954.

(56) Sheldrick, G. M. *Acta Crystallogr., Sect. A* **2008**, *64*, 112–122.

The Sc_2O cluster inside the C_{82} cage is disordered. Three orientations where found. The geometrical data for the minor clusters is less reliable than those of the set {Sc1, Sc2, O1} which has the highest occupancy (38%) and gave the clearest indication of the oxygen position. Some residual electron density resides inside the C_{82} cage and probably represents very minor, additional positions for the Sc_2O group. The Sc and O occupancies were freely refined and subsequently fixed.

The hydrogen atoms were generated geometrically and refined as riding atoms with C−H distances = 0.95−0.99 Å and U_{iso}(H) = 1.2 times U_{eq}(C) for CH and CH_2 groups and U_{iso}(H) = 1.5 times U_{eq}(C) for CH_3 groups. The maximum and minimum peaks in the final difference Fourier map were 1.229 and −0.911 eÅ^{-3}.

Crystal data: $C_{131.4}H_{55.8}N_4NiO_2Sc$, M_w = 1858.06 amu, monoclinic, *C*2/*m*, a = 25.3421(6) Å, b = 14.7875(4) Å, c = 20.3492(5) Å, β = 96.447(2)°, V = 7577.6(3) Å^3, T = 100(2) K, Z = 4, d_{calc} = 1.629 g/cm^3, R_1 [$I > 2\sigma$ (I)] = 0.0748, wR_2 (all data) = 0.2147, GOF (on F^2) = 1.017.

Computational Details. The calculations were carried out by using DFT methodology with the ADF 2007 package.[57] The exchange-correlation functionals of Becke[58] and Perdew[59] were used. Relativistic corrections were included by means of the ZORA formalism. Slater TZP basis sets were employed to describe the valence electrons of C, O and Sc. Frozen cores consisting of the 1s shell for C and N and the 1s to 2p shells for Sc were described by means of single Slater functions. B3LYP calculations have been carried using a GTO TZP basis set by means of the TURBOMOLE package.

Acknowledgment. We thank the National Science Foundation (Grants CHE-0716843 to ALB and MMO, CHE-0547988 to SS), the DOE GAANN Fellowship (P200A060323 to SS), the Lucas Research Foundation for financial support and the Advanced Light Source, supported by the Director, Office of Science, Office of Basic Energy Sciences, of the U.S. Department of Energy under Contract No. DE-AC02-05CH11231, for beam time, and Dr. Simon J. Teat and Dr. Christine M. Beavers for their assistance. B.Q.M. thanks the United States Department of Education for a GAANN Fellowship. This work was also supported by the Spanish Ministry of Science and Innovation [Project Ns. CTQ2008-06549-C02-01/BQU and the Ramón y Cajal Program (ARF)] and by the DURSI of the Generalitat de Catalunya (2009SGR462 and XRQTC).

Supporting Information Available: Computational details and results. X-ray crystallographic files in CIF format for $Sc_2(\mu_2\text{-}O)@C_s(6)\text{-}C_{82}\cdot Ni(OEP)\cdot 1.4CH_3C_6H_5\cdot 0.6C_6H_6$. Complete ref 41a. This material is available free of charge via the Internet at http://pubs.acs.org.

JA104902E

(57) ADF 2007 01, Department of Theoretical Chemistry; Vrije Universiteit: Amsterdam.
(58) Becke, A. D. *Phys. Rev. A* **1988**, *38*, 3098–3100.
(59) Perdew, J. P. *Phys. Rev. B* **1986**, *33*, 8822–8824.